Topochemical Photoreaction of Unsymmetrically Substituted Diolefins. 3. Photochemical Behavior of 4-[2-(2-Pyrazyl)ethenyl]styrene Derivative Crystals

Masaki Hasegawa,* Masato Aoyama, Yasunari Maekawa, and Yuji Ohashi†

Department of Synthetic Chemistry, Faculty of Engineering, The University of Tokyo, Hongo, Bunkyo-ku, Tokyo, 113, Japan, and Department of Chemistry, Faculty of Science, Ochanomizu University, Otsuka, Bunkyo-ku, Tokyo, 112, Japan. *Received May 18, 1988*

ABSTRACT: The photochemical behaviors in the crystalline state of methyl and ethyl 4-[2-(2-pyrazyl)-ethenyl]cinnamates (**3** and **4**), methyl α-cyano-4-[2-(2-pyrazyl)ethenyl]cinnamate (**5**), β-cyano-4-[2-(2-pyrazyl)ethenyl]stilbene (**6**), and 4-[2-(2-pyrazyl)ethenyl]chalcone (**7**) were studied. These monomers underwent topochemical photoreactions to give products having cyclobutane rings in the main chain; **3** and **4** showed very high photoreactivity and gave high molecular weight crystalline linear polymers with a recurring 1,3-*trans*-cyclobutane ring in the main chain; **5**, **6**, and **7** gave the oligomers having a zigzag-type main chain. X-ray crystal analysis of **4** showed that the molecules in the crystal were packed in the α-type arrangement usually seen in the photopolymerizable diolefins.

[2 + 2] photocyclodimerization of olefinic crystals is one of the most intensively studied topochemical reactions. The reaction has been widely applied to the cycloaddition polymerization of diolefinic crystals, which is called "four-center-type photopolymerization".[1]

Recently, we reported the topochemical photoreaction of several unsymmetrically substituted diolefin crystals, in which the reactivity and the structure of the products drastically vary with a slight modification of chemical structure.[2]

The cyclobutane rings in the photoproducts are classified into two types depending on the crystal structure of the monomer; the heteroadduct type and the homoadduct type. The former type of cyclobutane is formed by reacting two olefins having different substituents, while the latter type is obtained from olefins having the same substituents. For example, the photoreaction of methyl 4-[2-(4-pyridyl)ethenyl]cinnamate, ethyl α-cyano-4-[2-(4-pyridyl)ethenyl]cinnamate, and methyl α-cyano-4-[2-(2-pyridyl)ethenyl]cinnamate crystals gave a linear heteroadduct polymer, a linear homoadduct polymer, and a heteroadduct zigzag type of dimer, respectively.

Diolefin molecules having a pyrazyl ring, which is a stronger electron-withdrawing group than the pyridyl ring, are expected to be arranged in the crystal differently from the analogous pyridyl compounds and to afford different photoproducts.

As part of exploratory work to establish the correlation between the chemical structure and the molecular arrangement in diolefin crystals, we report here on the photoreaction of the unsymmetrically substituted diolefin compounds with a terminal pyrazyl ring (**3**–**7**).

Experimental Section

Measurements. Infrared spectra were recorded on a JASCO IR-810 spectrophotometer, and ^{1}H NMR spectra were obtained by using JEOL PMX-60SI and JEOL GX-400 instruments. The X-ray diffraction pattern was recorded on a RIGAKU Rotaflex RU-200 spectrometer (λ = 1.541 84 Å). Melting points were determined by a Laboratory Devices MEL-TEMP and are uncorrected. Gel permeation chromatography (GPC) of the photoproduct was performed at 40 °C on a Toyo Soda TSK-GEL (G2500HXL + G3000HXL) column (THF solution) or Shodex (GPC AD 800/P + AD 805/S + AD 803/S + AD 802/S + AD 802/S) column (DMF solution).

Synthesis of Monomers. 4-[2-(2-Pyrazyl)ethenyl]benzaldehyde (1). Terephthalaldehyde (16.8 g, 125 mmol) was dissolved in a mixed solvent of acetic anhydride (125 mmol) and acetic acid (125 mmol) at 70 °C. 2-Methylpyrazine (9.4 g, 100 mmol) was added to the solution and refluxed for 20 h. After the solution cooled to room temperature, benzene (500 mL) was added and extracted with 12 M hydrochloric acid (1500 mL), followed by neutralization with sodium hydrogen carbonate. The precipitates were collected by filtration. To the precipitates, dichloromethane (1000 mL) was added and stirred for 30 min. The solution was filtered and concentrated under reduced pressure. The solid mass was purified by flash column chromatography (Wako gel C-300, eluent dichloromethane:methanol = 99:1 (v/v)) to give crude **1** which was further purified by sublimation, followed by recrystallization from hexane. Yield 50%. Mp 122.5–124.0 °C (hexane). IR (KBr) 2850, 1690, 1635, 1400, 970 cm^{-1}. NMR ($CDCl_3$): δ 10.0 (formyl, s, 1 H), 8.70 (pyrazyl, d, 1 H, J = 1 Hz), 8.60 (pyrazyl, dd, 1 H, J = 1, J' = 2 Hz), 8.50 (pyrazyl, d, 1 H, J = 2 Hz), 7.93 (phenylene, d, 2 H, J = 8 Hz), 7.86 (olefin, d, 1 H, J = 16 Hz), 7.76 (phenylene, d, 2 H, J = 8 Hz), 7.29 (olefin, d, 1 H, J = 16 Hz). Anal. Calcd. for $C_{13}H_{10}N_2O$: C, 74.26%; H, 4.80%; N, 13.33%. Found: C, 74.54%; H, 4.74%; N, 13.27%.

4-[2-(2-Pyrazyl)ethenyl]cinnamic Acid (2). To a solution of **1** (10.5 g, 50 mmol) in pyridine (60 mL) were added malonic acid (15.6 g, 150 mmol) and piperidine (0.1 mL), and the solution was refluxed for 8 h. After cooling to room temperature, the solution was poured into water (200 mL). The precipitate was collected by filtration and washed with water. The filtrate was neutralized with 2 M hydrochloric acid and the precipitate collected by filtration and washed. Both precipitates were combined, dried under reduced pressure at 40 °C for 6 h, and recrystallized from methanol. Yield 96%. Mp 265 °C (dec.). IR (KBr) 1695, 1635, 1400, 975 cm^{-1}. NMR (DMSO-d_6) δ 12.4 (acid, br s, 1 H), 8.81 (pyrazyl, d, 1 H, J = 1.4 Hz), 8.64 (pyrazyl, dd, 1 H, J = 1.4, J' = 2.3 Hz), 8.51 (pyrazyl, d, 1 H, J = 2.3 Hz), 7.80 (olefin, d, 1 H, J = 16.0 Hz), 7.75 (phenylene, s, 4 H), 7.61 (olefin, d, 1 H, J = 16.0 Hz), 7.49 (olefin, d, 1 H, J = 16.0 Hz), 6.59 (olefin, d, 1 H, J = 16.0 Hz). Anal. Calcd. for $C_{15}H_{12}N_2O_2$: C, 71.42%; H, 4.76%; N, 11.11%. Found: C, 71.50%; H, 4.81%; N, 11.09%.

3 and 4. To a suspension of **2** (5.0 g, 2 mmol) in methanol (70 mL) was added concentrated sulfuric acid (0.5 mL), and the mixture was refluxed for an hour to give a homogeneous solution. After cooling to room temperature, the solution was neutralized with 1 M aqueous sodium hydroxide solution and extracted with chloroform (300 mL). Evaporation of the solvent and purification by column chromatography (Wako gel C-200, eluent was chloroform) gave **3**, which was recrystallized from methanol. Yield 93%. Mp 170.0–171.0 °C (methanol). IR (KBr) 1705, 1635, 1395, 985 cm^{-1}. NMR ($CDCl_3$) δ 8.65 (pyrazyl, s, 1 H), 8.56 (pyrazyl,

*Address correspondence to this author at The University of Tokyo.
†Ochanomizu University.

0024-9297/89/2222-1568$01.50/0

s, 1 H), 8.43 (pyrazyl, s, 1 H), 7.75 (olefin, d, 1 H, J = 16.5 Hz), 7.68 (olefin, d, 1 H, J = 16.5 Hz), 7.61 (phenylene, d, 2 H, J = 8.5 Hz), 7.56 (phenylene, d, 2 H, J = 8.5 Hz), 7.24 (olefin, d, 1 H, J = 16.1 Hz), 6.47 (olefin, d, 1 H, J = 16.1 Hz), 3.95 (ester, s, 3 H). Anal. Calcd for $C_{16}H_{14}N_2O_2$: C, 72.15%; H, 5.31%; N, 10.52%. Found: C, 72.23%; H, 5.17%; N, 10.30%.

In a similar manner, **2** was esterified with ethanol to give **4** in 85% yield. Mp 156.5–157.0 °C (ethanol). IR (KBr) 1705, 1635, 1395, 985 cm^{-1}. NMR ($CDCl_3$) δ 8.65 (pyrazyl, s, 1 H), 8.56 (pyrazyl, s, 1 H), 8.43 (pyrazyl, s, 1 H), 7.75 (olefin, d, 1 H, J = 16.5 Hz), 7.68 (olefin, d, 1 H, J = 16.5 Hz), 7.61 (phenylene, d, 2 H, J = 8.5 Hz), 7.56 (phenylene, d, 2 H, J = 8.5 Hz), 7.24 (olefin, d, 1 H, J = 16.1 Hz), 6.47 (olefin, d, 1 H, J = 16.1 Hz), 4.28 (ester, q, 2 H, J = 7.3 Hz), 1.35 (ester, t, 3 H, J = 7.3 Hz). Anal. Calcd for $C_{17}H_{16}N_2O_2$: C, 72.83%; H, 5.76%; N, 9.99%. Found: C, 73.04%; H, 5.70%; N, 9.98%.

5–7. To a solution of **1** (2.1 g, 100 mmol) in methanol (80 mL) were added methyl cyanoacetate (1.33 g, 135 mmol) and piperidine (0.5 mL), and the mixture was stirred at room temperature for 7 h. The resulting yellow precipitate was collected by filtration and washed with a small amount of methanol. Recrystallization from methanol gave **5**. Yield 88%. Mp 193.0–194.0 °C (dec.). IR (KBr) 2230, 1735, 1630, 980 cm^{-1}. NMR ($CDCl_3$) δ 8.68 (pyrazyl, d, 1 H, J = 1.5 Hz), 8.59 (pyrazyl, dd, 1 H, J = 1.5, J' = 2.4 Hz), 8.47 (pyrazyl, d, 1 H, J = 2.4 Hz), 8.26 (olefin, s, 1 H), 8.05 (phenylene, d, 2 H, J = 8.5 Hz), 7.80 (olefin, d, 1 H, J = 16.2 Hz), 7.72 (phenylene, d, 2 H, J = 8.5 Hz), 7.30 (olefin, d, 1 H, J = 16.2 Hz), 3.95 (ester, s, 3 H). Anal. Calcd for $C_{17}H_{13}N_3O_2$: C, 70.08%; H, 4.51%; N, 14.43%. Found: C, 70.34%; H, 4.34%; N, 14.46%.

Similar condensations of **1** with benzyl cyanide and acetophenone gave **6** and **7**, respectively.

6: Mp 153.0–154.0 °C (ethanol). IR (KBr) 2230, 1635, 1610, 985 cm^{-1}. NMR ($CDCl_3$) δ 8.66 (pyrazyl, d, 1 H, J = 1.5 Hz), 8.57 (pyrazyl, dd, 1 H, J = 1.5, J' = 2.4 Hz), 8.44 (pyrazyl, d, 1 H, J = 2.4 Hz), 7.94 (phenyl, d, 2 H, J = 8.6 Hz), 7.78 (olefin, d, 1 H, J = 16.2 Hz), 7.71–7.67 (phenyl, phenylene, m, 4 H), 7.53 (olefin, s, 1 H), 7.48–7.38 (phenyl, m, 3 H), 7.24 (olefin, d, 1 H, J = 16.2 Hz). Anal. Calcd for $C_{21}H_{15}N_3$: C, 81.52%; H, 4.90%; N, 13.58%. Found: C, 81.58%; H, 4.71%; N, 13.50%.

7: Mp 159.0–160.0 °C (water–acetonitrile 1:1 (v/v)). IR (KBr) 1665, 1635, 985 cm^{-1}. NMR ($CDCl_3$) δ 8.82 (pyrazyl, d, 1 H, J = 1.1 Hz), 8.65 (pyrazyl, dd, J = 1.1, J' = 2.1 Hz), 8.52 (pyrazyl, d, 1 H, J = 2.1 Hz), 8.18 (phenyl, d, 2 H, J = 7.3 Hz), 8.01 (olefin, d, 1 H, J = 15.6 Hz), 7.97 (phenylene, d, 2 H, J = 7.9 Hz), 7.83 (olefin, d, 1 H, J = 16.2 Hz), 7.80 (phenylene, d, 2 H, J = 7.9 Hz), 7.77 (olefin, d, 1 H, J = 15.6 Hz), 7.68 (phenyl, t, 2 H, J = 7.3 Hz), 7.59 (phenyl, t, 1 H, J = 7.3 Hz), 7.54 (olefin, d, 1 H, J = 16.2 Hz). Anal. Calcd for $C_{21}H_{16}N_2O$: C, 80.74%; H, 5.17%; N, 8.97%. Found: C, 80.66%; H, 5.10%; N, 8.94%.

Photoreaction Conditions. Method 1. Crystals of **3** and **4** in a sample tube under nitrogen atmosphere were irradiated with a 500-W super-high-pressure mercury lamp (USHIO USH-500D). **Method 2.** Finely powdered crystals of **4–7** (100–200 mg) were dispersed in 250 mL of H_2O containing a few drops of surfactant (NIKKOL TL-10FF) and with rigorous stirring under a nitrogen atmosphere were irradiated with a 100-W high-pressure mercury lamp (EIKOSHA EHB WF-100) through an uranium glass filter.

X-ray Measurement. The single crystal was grown from an ethanol solution. Preliminary photographic X-ray examination established the crystal system and approximate cell dimensions. A crystal (0.8 × 0.3 × 0.1 mm) was mounted on a Rigaku four-circle diffractometer equipped with Cu Kα radiation and graphite monochromator (40 kV, 20 mA, λ = 1.541 84 Å). Accurate cell dimensions were obtained by least-squares refinement of 16 accurately centered reflections in the range 40° < 2θ < 60°. The intensities were measured in the range 2θ < 125° by the ω–2θ scan, with a scanning rate of 4 deg (θ) min^{-1} and scan range of (1.0 + 0.15 tan θ) deg. Stationary background counts were accumulated for 5 s before and after each scan. An intensity variation between 0.961 and 1.005 was noted in the three check reflections (6 4 0), (−10 0 2), and (5 0 4) during the data collection. There were 2318 unique reflections observed, of which 1976 with $|F_o| > 3\sigma(|F_o|)$ were used in the solution and refinement; no absorption correction was made. The structure was solved by direct method with the MULTAN 78 program and refined by full-matrix least-squares method with SHELX 76. No peaks higher than 0.3 e Å^{-3} were found in the final difference electron density synthesis. The final R and R_w values obtained were 0.072 and 0.107, respectively, for 1976 reflections; $w = [\sigma(|F_o|)^2 + 0.019272(|F_o|)^2]^{-1}$.

Measurement of Unit Cell Dimensions. The unit cell dimensions of the polymer were determined by the spacing of the $hk0$ reflections recorded on Weissenberg photographs and the hkl reflections on oscillation photographs (Figure 7).

The single crystal of the monomer was mounted on the goniometer head. Oscillation and Weissenberg photographs were taken for reference before irradiation. When the rotating crystal was irradiated with 100-W high-pressure mercury lamp for 2 h, the photographs of partially polymerized crystal were taken.

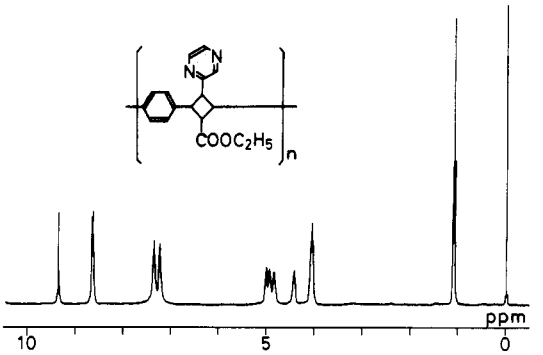

Figure 1. 400-MHz ^{1}H NMR spectrum of poly-**4** obtained by lyophilizing the polymer HFIP solution.

Results and Discussion

Photoreaction of 3 and 4. Diolefins **3** and **4** showed a very high photoreactivity in the crystalline state; the reaction proceeded quickly even in sunlight. On irradiation, IR absorptions at 1630 and 970 cm^{-1} due to olefinic double bonds gradually decreased and finally disappeared. The absorption of the ester shifted by 10 cm^{-1} to higher wavenumber. Inherent viscosities of the photoproducts (poly-**3**, poly-**4**) obtained from **3** and **4** by irradiation for 5 h with a 500-W super-high-pressure mercury lamp (method 1) reached values as high as 3.93 and 8.19 dL/g (1,1,1,3,3,3-hexafluoro-2-propanol (HFIP) solution, 0.30 g/dL, 30 °C), respectively. Poly-**4** obtained by irradiation for 8 h with a 100-W high-pressure mercury lamp (method 2) had an inherent viscosity of 6.83 dL/g (HFIP solution, 0.30 g/dL, 30 °C). In the ^{1}H NMR spectrum (CF_3COOD solution obtained by lyophilizing the polymer HFIP solution), no olefinic protons were observed, but the four kinds of methyne protons bonded to cyclobutane appeared, indicating the occurrence of the four-center-type photopolymerization (Figure 1: δ 9.36, 8.66, and 8.63, pyrazyl; 7.35 and 7.23, phenylene; 5.00, 4.93, 4.83, and 4.42, cyclobutane; 4.05 and 1.10, ester). Outstanding sharpness of all the peaks in this spectrum indicates that the photoproduct has little defect in chemical structure. In the ^{1}H J-correlated two-dimensional (COSY) NMR spectrum of this product, each proton of the cyclobutane has two cross peaks, indicating the heteroadduct structure as shown in Scheme Ia. If any formation of the homoadduct structure occurs, each proton of the cyclobutane should exhibit only one cross peak. The X-ray diffraction pattern of poly-**4** (Figure 2) is of high crystallinity. Monomer **3** showed nearly the same spectral changes on photoirradiation and gave the highly crystalline polymer. As **3** and poly-**3** exhibited the same NMR and IR spectra and similar X-ray patterns to those of **4** and poly-**4**, respectively, the photoreaction of **3** is doubtlessly the same type of crystal-to-crystal transformation as **4**. Such remarkably large values of viscosity (8.19) and high crystallinity of the photoproducts are the first example for a polymer obtained from

Scheme I

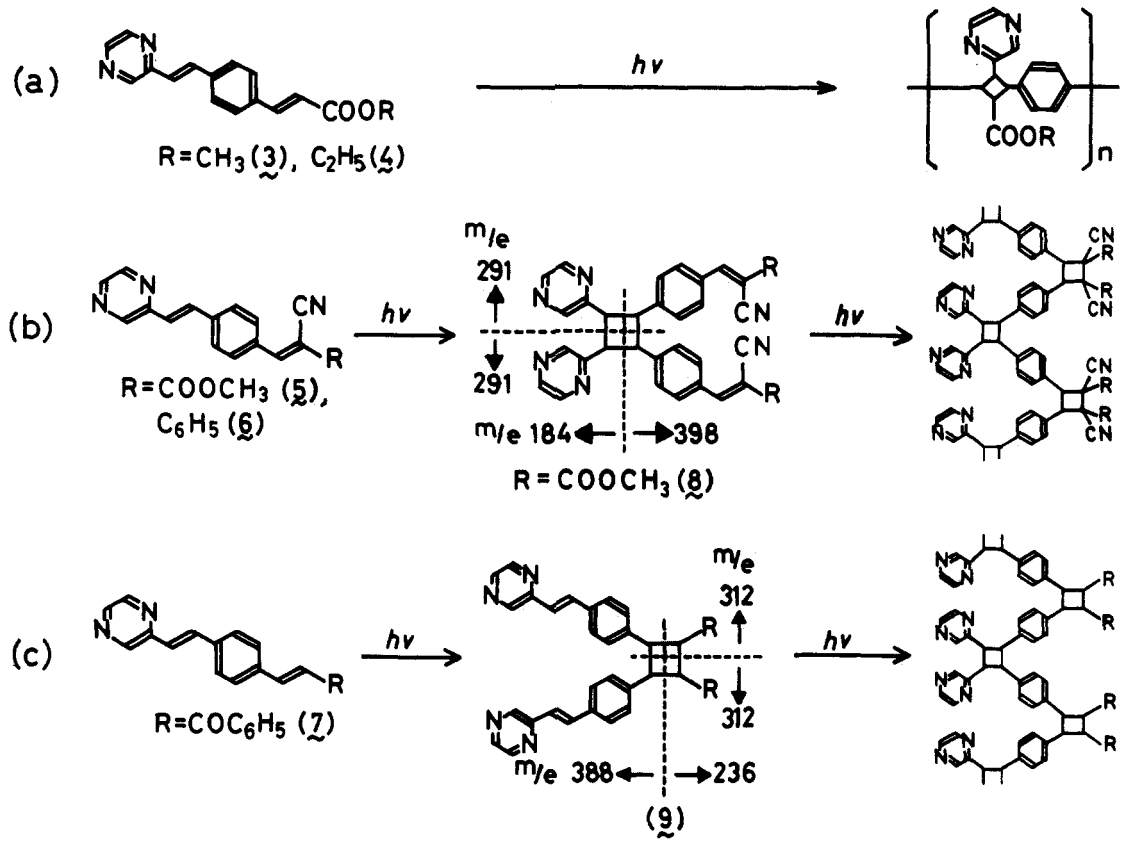

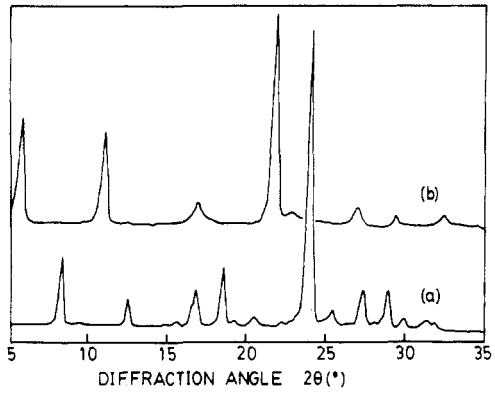

Figure 2. X-ray diffraction pattern of (a) 4 and (b) its polymer.

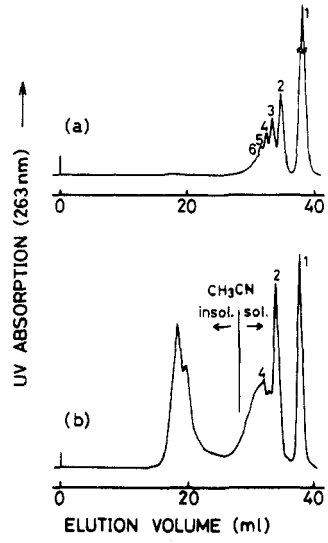

Figure 3. GPC curves of the photoproduct in DMF solution. (a) DMF-soluble part of the photoproduct of 4 after irradiation for 3.5 h with a 500-W super-high-pressure mercury lamp, cutting off the wavelength shorter than 355 nm. (b) The photoproduct of 7 after irradiation for 2 h with high-pressure mercury lamp.

the unsymmetrically substituted diolefin compounds.

In order to observe the chain growth during the reaction, 4 was irradiated for 3.5 h with a 500-W super-high-pressure mercury lamp ($\lambda > 355$ nm), thus enabling excitation of only the monomer and preventing further photoreaction of terminal olefin groups. The GPC (DMF solution) curve of the DMF-soluble portion (Figure 3a) shows the consecutive formation of the dimer, trimer, tetramer, and higher oligomers, indicating a typical step-growth polymerization mechanism.

Photoreaction of 5 and 6. Due to the lower photoreactivity of 5 compared with that of 3 and 4, more prolonged irradiation (>24 h) was required to complete the reaction when powdered crystals of 5 were dispersed in water, stirred, and irradiated with a 100-W high-pressure mercury lamp (method 2). The photoproduct was amorphous, its molecular weight was estimated as 3.8×10^3, and M_w/M_n was 1.4 by GPC (THF solution). The absorption of the cyano group shifted to higher wavenumber (2230 → 2240 cm^{-1}), in addition to similar absorption changes to those observed in 3 and 4. In the GPC curve of the product irradiated for 7.5 h, a large amount of polymeric products with a broader molecular weight distribution was seen, in addition to the monomer and dimer, trimer, and tetramer. The mass spectrum of the dimer (isolated from the product mixture by column chromatography) showed peaks at 398 and 184 due to the asymmetric cleavage of the cyclobutane ring which is a homoadduct head-to-head type between two 2-pyrazyl ethenyl groups; in addition, peaks corresponding to the dimer at 582 (M^+) and the monomer at 291 ($M^+/2$) were observed (Scheme Ib). This result indicates that the dimer structure is 1,2-bis(2-pyrazyl)-3,4-bis[4-(2-cyano-2-(meth-

oxycarbonyl)ethenyl)phenyl]cyclobutane (8) and was supported by ^{1}H NMR ($CDCl_3$) analysis; that is, the olefinic protons on the pyrazyl side at δ 7.80 and 7.30 in the monomer disappeared in the dimer while that of the cinnamate group at δ 8.26 shifted to 8.14. Moreover, the cyclobutane protons of the dimer appeared as an AA'BB' pattern at δ 5.03 and 4.73 ($J_{AA'} = J_{BB'} = 10.3$, $J_{AB} = J_{A'B'} = 6.3$, $J_{AB'} = J_{A'B} = 0.0$ Hz). The dimer structure indicates that the molecular arrangement in the crystal of **5** is a fully overlapped β-type packing. Therefore, **5** gave a homoadduct-type head-to-head dimer, presumably followed by subsequent formation of zigzag oligomers as shown in Scheme Ib. At the latter stage of the photoreaction, the topochemical environment gradually deteriorated, resulting in a considerable amount of indefinable polymeric substances. Thus, in order to facilitate the reaction, a larger movement may be required of the molecules in the β-type arrangement, compared with those in the α-type.

The photoreaction of **6** was carried out under the same conditions as for **5**. The photoreactivity and IR spectral change of **6** during the reaction are similar to those of **5**. The molecular weight of the photoproduct was estimated as 3.3×10^3 ($M_w/M_n = 1.4$) by GPC analysis, and the ^{1}H NMR spectrum of the dimer in the cyclobutane region was the same as that of **5**. These results indicate that the photoreaction of **6** was of the same type as that of **5**.

Photoreaction of 7. As several chalcone-derived crystals are known to undergo [2 + 2] topochemical photoreactions,[3] the chalcone group was introduced as one olefin component in the diolefin derivatives to see if the chalcone group plays an influencing role in topochemical molecular arrangement. The monomer **7** was highly photoreactive and disappeared completely after the irradiation for 4 h in water with a 100-W high-pressure mercury lamp (method 2). The GPC curve of the product irradiated for 2 h showed the formation of dimer, oligomer, and indefinable polymeric substances (Figure 3b); the molecular weight of the oligomer sample was estimated as 2.3×10^3 ($M_w/M_n = 1.5$). The mass spectrum of the dimer (isolated by column chromatography) showed peaks at 388 and 236 due to asymmetric cleavage of the homoadduct head-to-head type cyclobutane ring between two benzoyl ethenyl groups, in addition to the peaks at 624 (M^+) and 312 ($M^+/2$) (symmetric cleavage of the cyclobutane). The dimer structure was supported by the ^{1}H NMR spectrum and thus concluded to be 1,2-dibenzoyl-3,4-bis[4-(2-(2-pyrazyl)ethenyl)phenyl]cyclobutane (**9**). On the basis of the dimer structure, the crystal structure of **7** is assumed to be the β-type which initially should give a homoadduct head-to-head dimer (**9**) and subsequently a zigzag polymer, as shown in Scheme Ic. It is noteworthy that the first cyclodimerization occurs between two olefinic bonds at the pyrazyl side in **5** and **6**, but at the benzoyl side in **7**.

The photoproduct of **7** (GPC cure in Figure 3b) was separated into two parts by solubility difference in acetonitrile. Monomer and oligomers, of which the degree of polymerization is approximately 2–7, were found in the acetonitrile-soluble part, whereas the acetonitrile-insoluble portion consisted mainly of polymeric product. It is most likely that the topochemical reaction occurred only at the oligomerization stage, followed by subsequent nontopochemical miscellaneous reactions.

Molecular Structure. The crystallographic data of **4** are $M_r = 280.33$, monoclinic, $P2_1/c$, $a = 20.834$ (2), $b = 9.479$ (1), $c = 7.387$ (0) Å, $\beta = 96.75$ (1)°, $V = 1448.7$ (2) Å^3, $Z = 4$, $F(000) = 592$, $D_X = 1.285$ g·cm^{-3}, $\mu = 6.06$ cm^{-1}.

The molecular structure and atom numbering system of **4** are shown in Figure 4. Atomic and thermal parameters are listed in Table I. Bond lengths and angles are shown in Table II. The C(6)–C(7)–C(8) angle (126.0°), C(7)–C(8)–C(9) angle (127.7°), C(8)–C(9)–C(14) angle (123.6°), C(12)–C(15)–C(16) angle (127.8°) and C(16)–C(17)–C(18) angle (124.3°) are considerably larger than the sp^2 angle.

The benzene and pyrazine rings and ethylene group are planar within experimental errors. To the pyrazyl side of

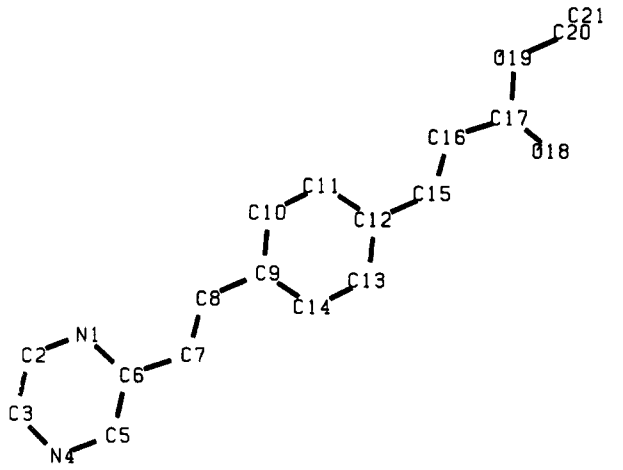

Figure 4. Molecular structure of **4** with the atom numbering scheme.

Table I
Final Atomic Coordinates (×10^4 for C, N, and O; ×10^3 for H) with Equivalent Isotropic Thermal Parameters, B_{eq} (Å^2), for Non-Hydrogen Atoms and Isotropic Thermal Parameters, B (Å^2), for Hydrogen Atoms for 4

$$B_{eq} = \frac{1}{3}\sum_i\sum_j B_{ij}a_i^*a_j^*a_ia_j$$

atom	x	y	z	B_{eq} or B
O(1)	1123 (1)	1016 (5)	4470 (2)	4.1 (1)
C(2)	712 (1)	1977 (7)	4430 (2)	3.4 (1)
C(3)	−1016 (1)	−904 (7)	608 (3)	3.9 (1)
C(4)	437 (1)	522 (7)	3432 (2)	3.0 (1)
C(5)	658 (1)	−1504 (7)	2698 (2)	3.3 (1)
C(6)	10 (1)	1243 (7)	3274 (2)	3.3 (1)
C(7)	−750 (1)	1438 (8)	2459 (3)	3.9 (1)
C(8)	−597 (1)	−1931 (8)	514 (3)	4.3 (1)
C(9)	−1353 (1)	−1561 (8)	−357 (3)	4.2 (1)
C(10)	−2074 (1)	−1001 (8)	−1480 (3)	4.2 (1)
C(11)	−2492 (1)	188 (10)	−1470 (3)	4.9 (1)
O(12)	580 (1)	3833 (6)	5106 (2)	4.8 (1)
C(13)	−1085 (1)	775 (8)	1603 (3)	4.4 (1)
C(14)	−327 (1)	362 (7)	2347 (2)	3.2 (1)
C(15)	−259 (1)	−1295 (8)	1347 (3)	3.9 (1)
N(16)	842 (1)	−3173 (7)	2136 (2)	5.0 (1)
C(17)	−1996 (1)	−2617 (10)	−2470 (3)	5.1 (1)
C(18)	−1752 (1)	−393 (9)	−483 (3)	4.5 (1)
N(19)	−2730 (1)	−1812 (8)	−3357 (3)	5.8 (1)
C(20)	1427 (1)	2463 (12)	5371 (4)	5.1 (1)
C(21)	−2334 (1)	−2995 (11)	−3370 (3)	5.8 (1)
C(22)	−2800 (1)	−252 (11)	−2394 (3)	5.6 (1)
H(6)	−9 (1)	259 (9)	381 (3)	4.4 (7)
H(7)	−80 (1)	247 (9)	320 (3)	4.5 (7)
H(8)	56 (1)	−710 (10)	14 (4)	5.8 (9)
H(9)	126 (1)	−683 (11)	100 (4)	7.5 (11)
H(11)	256 (1)	−128 (9)	75 (3)	5.3 (8)
H(13)	−134 (1)	142 (10)	178 (3)	6.0 (9)
H(15)	6 (1)	−194 (9)	122 (3)	5.3 (8)
H(17)	173 (1)	350 (10)	254 (4)	6.3 (9)
H(18)	183 (2)	−1099 (13)	−33 (4)	7.9 (11)
H(20)$_1$	168 (2)	128 (11)	537 (4)	7.0 (11)
H(20)$_2$	124 (2)	251 (15)	601 (5)	10.7 (16)
H(20)$_3$	147 (2)	474 (14)	517 (4)	7.5 (11)
H(21)	228 (1)	412 (10)	405 (3)	5.6 (8)
H(22)	313 (1)	−65 (11)	244 (4)	7.2 (10)

Table II
Bond Distances and Angles for 4

	bond length, Å		bond angle, deg
N(1)–C(2)	1.321 (4)	C(2)–N(1)–C(6)	115.8 (3)
N(1)–C(6)	1.349 (3)	N(1)–C(2)–C(3)	123.5 (3)
C(2)–C(3)	1.353 (5)	C(2)–C(3)–N(4)	122.5 (3)
C(3)–N(4)	1.336 (5)	C(3)–N(4)–C(5)	114.9 (3)
N(4)–C(5)	1.337 (5)	N(4)–C(5)–C(6)	123.0 (3)
C(5)–C(6)	1.391 (4)	N(1)–C(6)–C(5)	120.4 (3)
C(6)–C(7)	1.463 (4)	N(1)–C(6)–C(7)	118.2 (2)
C(7)–C(8)	1.332 (4)	C(5)–C(6)–C(7)	121.5 (3)
C(8)–C(9)	1.462 (4)	C(6)–C(7)–C(8)	123.4 (3)
C(9)–C(10)	1.388 (4)	C(7)–C(8)–C(9)	127.7 (3)
C(9)–C(14)	1.395 (4)	C(8)–C(9)–C(10)	118.8 (2)
C(10)–C(11)	1.373 (5)	C(8)–C(9)–C(14)	123.6 (3)
C(11)–C(12)	1.404 (4)	C(10)–C(9)–C(14)	117.6 (3)
C(12)–C(13)	1.389 (4)	C(9)–C(10)–C(11)	121.7 (3)
C(12)–C(15)	1.464 (4)	C(10)–C(11)–C(12)	121.0 (3)
C(13)–C(14)	1.384 (5)	C(11)–C(12)–C(13)	117.3 (3)
C(15)–C(16)	1.319 (5)	C(11)–C(12)–C(15)	123.1 (3)
C(16)–C(17)	1.471 (5)	C(13)–C(12)–C(15)	119.6 (3)
C(17)–O(18)	1.205 (5)	C(12)–C(13)–C(14)	121.5 (3)
C(17)–O(19)	1.345 (5)	C(9)–C(14)–C(13)	120.9 (3)
O(19)–C(20)	1.463 (7)	C(12)–C(15)–C(16)	127.8 (3)
C(20)–C(21)	1.432 (9)	C(15)–C(16)–C(17)	121.4 (3)
		C(16)–C(17)–O(18)	124.3 (3)
		C(16)–C(17)–O(19)	110.8 (3)
		O(18)–C(17)–O(19)	124.9 (4)
		C(17)–O(19)–C(20)	117.2 (4)
		O(19)–C(20)–C(21)	109.6 (5)

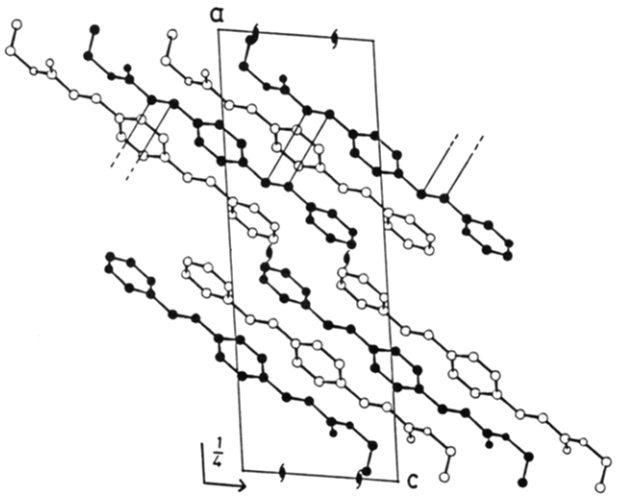

Figure 5. Crystal structure of 4 viewed along the *b* axis. The double bonds which form cyclobutanes are linked by solid lines.

the molecule in Figure 4, the benzene ring rotates 1.93° about C(8)–C(9) from the ethylenic plane, and the pyrazine ring rotates 9.87° about C(6)–C(7) in the same direction. To the ester side, the benzene ring rotates 2.04° about C(12)–C(15) from the ethylenic plane, and the carbonyl group rotates 11.10° about C(16)–C(17) in the same direction. As mentioned above, the molecular structure is identified to be essentially the same as the corresponding symmetrically substituted diolefinic compounds, 2,5-distyrylpyrazine (DSP) or diethyl 1,4-phenylenediacrylate.[4a-c]

Crystal Structure. The molecules are stacked with respect to each other along the *c* axis and are related by translation symmetry. These molecules slide in the direction of the *c* axis by half a molecule, which is defined as α-type packing, as shown in Figure 5.

The shortest intermolecular contact between ethylenic double bonds is found between the molecules related by the *c* translation. These double bonds approached each other with distances of 3.948 (4) Å for C(7)···C(15) and 3.953 (4) Å for C(8)···C(16) and are therefore approximately parallel. The next shortest contacts, which are greater than 5 Å, are not parallel and are found between the molecules related by the *c* glide.

It is most probable that the double bonds related by the *c* translation react to form a linear polymer with hetero-adduct cyclobutane rings with the same chirality. However, as all the asymmetric cyclobutanes in the next stack possess opposite chirality, the resulting polymer should be racemic. Actually the polymer obtained from a single

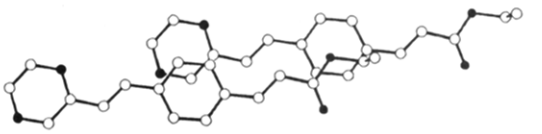

Figure 6. Overlapping of the reactive molecules viewed along the average normal to the benzene ring.

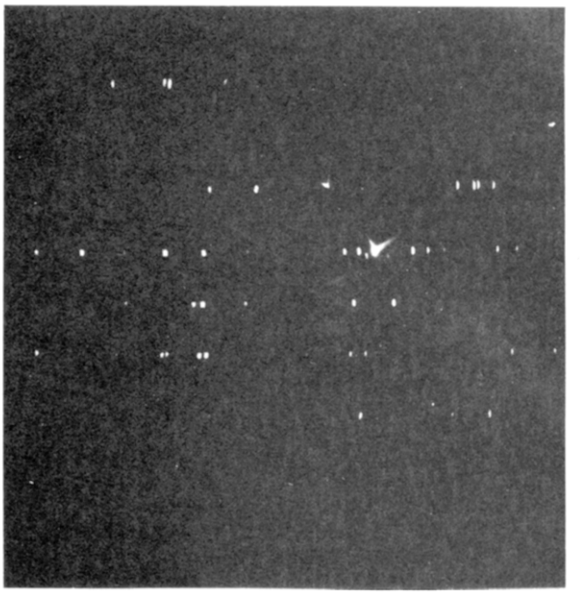

a

b

Figure 7. Oscillation photographs of 4 taken around the *c* axis: (a) before irradiation; (b) after irradiation for 2 h.

Table III
Crystallographic Data of Monomer 4, DSP, and P2VB

		a	*b*	*c*
4	monomer	20.834	9.479	7.387
	polymer	16.9 (−19%)	10.8 (14%)	7.80 (5.6%)
DSP	monomer	20.639	9.599	7.655
	polymer	18.4 (−11%)	10.9 (14%)	7.52 (−1.8%)
P2VB	monomer	21.060	9.567	7.311
	polymer	18.9 (−10%)	10.5 (10%)	7.53 (3.0%)

crystal shows neither optical rotation nor CD spectral changes.

There is no particularly short intermolecular contact. In Figure 6, the reacting molecules are projected in a plane normal to the benzene rings. The electron-rich pyrazyl ring, as well as the carbonyl oxygen atom, approach the electron-deficient benzene ring of a neighboring molecule. The same type of interaction has also been reported for several symmetric diolefin compounds.[4b,c]

Change of Crystal Structure with Polymerization. As shown in Figures 7 and 8, the reflections on the oscillation and Weissenberg photographs are extended as horizontal lines but the center of the lines coincide with the monomer axis. It is concluded that the polymer crystal is somewhat oriented, although the degree of orientation is small in comparison with those of DSP and 1,4-bis[2-(2-pyridyl)ethenyl]benzene (P2VB).[4a,d] The unit cell dimensions of both the monomer and the polymer are listed with the results of DSP and P2VB in Table III. The direction of polymer chain growth is parallel with the *c* axis in all cases. However, the change in length of the *c* axis is greater during the polymerization of **4** (5.6%) compared with those of DSP (−1.8%) and P2VB (3.0%). The length of the monomer repeating unit in the *c* axis of **4** is 7.387 Å, which is close to those of DSP (7.66 Å) and P2VB (7.31 Å). More extensive changes in the other two axial lengths are also similar to those of DSP and P2VB; the *a* axis is contracted by 19%, whereas the *b* axis is elongated by 14%. Thus, these results indicate that a high molecular weight crystalline polymer may be obtained even when there is a significant change in the axis of chain growth (*c* axis) during the polymerization.

Conclusions

The present photoreactivity study revealed that several new unsymmetrical diolefin crystals were photoreactive and that 2-(2-pyrazyl)ethenyl substituents were a topochemically potent component in the diolefin compounds. **3** and **4** gave high molecular weight crystalline linear polymers having a heteroadduct cyclobutane structure reflecting their α-type molecular arrangement in the monomer crystal. The configuration of the polymer, which was presumed from the crystal structure of **4**, was satisfactorily supported by IR and ^{1}H NMR spectral results. Even a significant change in the axis of chain growth may result in a highly crystalline linear high polymer. **5**, **6**, and **7** gave amorphous oligomers having a homoadduct-type cyclobutane structure. Substituting the cinnamate component of **3** for one of the α-cyanocinnamate (**5**), β-cyanostilbene (**6**), or chalcone (**7**) moieties causes a change in the molecular packing in the monomer crystal from the α-type to the β-type. Moreover, among the monomers with β-type packing, the first cyclodimerization in **5** and **7** occurs at different olefinic groups. In contrast to the diolefin compound of α-type packing, those of β-type packing undergo the topochemical reaction only in the early stage of the reaction, followed by a nontopochemical reaction in the latter stage, resulting in the formation of amorphous compounds.

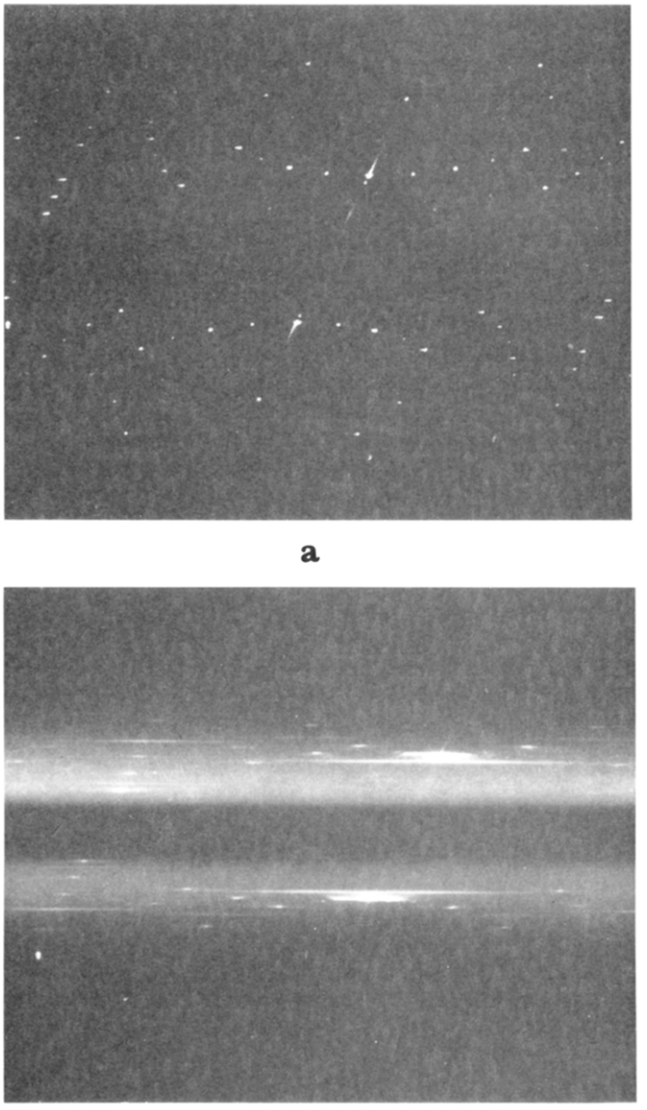

Figure 8. 0*kl* Weissenberg photographs of **4**: (a) before irradiation; (b) after irradiation for 2 h.

Registry No. **1**, 118356-67-5; **2**, 107139-60-6; **3**, 107130-91-6; poly-**3** (homopolymer), 112963-67-4; poly-**3** (SRU), 118375-55-6; **4**, 112963-68-5; poly-**4** (homopolymer), 112963-69-6; poly-**4** (SRU), 118356-68-6; **5**, 107130-94-9; **5** (homopolymer), 118356-69-7; **6**, 107131-00-0; **6** (homopolymer), 118356-70-0; **7**, 107131-03-3; terephthalaldehyde, 623-27-8; 2-methylpyrazine, 109-08-0; malonic acid, 141-82-2; methyl cyanoacetate, 105-34-0; benzyl cyanide, 140-29-4; acetophenone, 98-86-2.

Supplementary Material Available: Table containing thermal parameters for **4** (1 page). Ordering information is given on any current masthead page.

References and Notes

(1) Hasegawa, M. *Adv. Polym. Sci.* **1982**, *42*, 1; *Chem. Rev.* **1983**, *83*, 507.
(2) Results presented in part at a recent symposia; Hasegawa, M. *Pure Appl. Chem.* **1986**, *58*, 1179. Hasegawa, M.; Saigo, K.; Kato, S.; Harashina, H. *ACS Symp. Ser.* **1987**, *337*, 44. Hasegawa, M.; Harashina, H.; Kato, S.; Saigo, K. *Macromolecules* **1986**, *19*, 1276. Hasegawa, M.; Kato, S.; Yonezawa, N.; Saigo, K. *J. Polym. Sci., Part C, Polym. Lett. Ed.* **1986**, *24*, 153. Kato, S.; Nakatani, M.; Harashina, H.; Saigo, K.; Hasegawa, M.; Sato, S. *Chem. Lett.* **1986**, 847. Hasegawa, M.; Kato, S.; Saigo, K.; Wilson, S. R.; Stern, C. L.; Paul, I. C. *J. Photochem. Photobiol.* **1988**, *41*, 385.

(3) Rabinovich, D.; Schmidt, G. M. J. *J. Chem. Soc. B* **1970**, 6. Rabinovich, D. *J. Chem. Soc. B* **1970**, 11. Ohkura, K.; Kashino, S.; Haisa, M. *Bull. Chem. Soc. Jpn.* **1973**, *46*, 627. Kaftory, M.; Tanaka, K.; Toda, F. *J. Org. Chem.* **1985**, *50*, 2154. Hasegawa, M.; Saigo, K.; Mori, T.; Uno, H.; Nohara, M.; Nakanishi, H. *J. Am. Chem. Soc.* **1985**, *107*, 2788.

(4) (a) Nakanishi, H.; Hasegawa, M.; Sasada, Y. *J. Polym. Sci., Polym. Phys. Ed.* **1977**, *15*, 173. (b) Sasada, Y.; Shimanouchi, H.; Nakanishi, H.; Hasegawa, M. *Bull. Chem. Soc. Jpn.* **1971**, *44*, 1262. (c) Nakanishi, H.; Ueno, K.; Sasada, Y. *Acta Crystallogr., Sect. B* **1978**, *B34*, 2209. (d) Nakanishi, H.; Ueno, K.; Hasegawa, M.; Sasada, Y. *Chem. Lett.* **1972**, 301.

Direct Polarization ^{13}C and ^{1}H Magic Angle Spinning NMR in the Characterization of Solvent-Swollen Gels

H. D. H. Stöver and J. M. J. Fréchet*

Department of Chemistry, Cornell University, Ithaca, New York 14853-1301.
Received June 28, 1988; Revised Manuscript Received September 1, 1988

ABSTRACT: Direct polarization/magic angle spinning (DP/MAS) ^{13}C and ^{1}H NMR are shown to be well suited for the characterization of chemically modified cross-linked polymer gels. MAS is known to average out the residual motional anisotropies of the chain segments introduced by the cross-link points. At the same time, the ^{13}C direct polarization method exploits the rapid spin–lattice relaxation of the solvated chain segments to give good signal to noise for quaternary and protonated carbons alike.

Introduction

Functional groups on insoluble supports are as important as they are difficult to characterize. Our research work has frequently involved chemistry on solvent-swollen polystyrene beads,[1] which requires that reliable and facile NMR methods applicable to the gel state be available. Standard "solution-state" ^{1}H NMR[2,3] and especially ^{13}C NMR[4-6] have been used for swollen gels; the observed lines are, however, often broad due to the cross-link points, which restrict molecular motions of the chains.[7,8]

We have found high-field direct polarization/magic angle spinning (DP/MAS) ^{13}C and ^{1}H NMR to be well suited for the characterization of functionalized polystyrene beads swollen in deuteriochloroform. MAS averages out the residual motional anisotropy caused by the cross-link points, while the direct polarization method, in contrast to recently reported crosspolarization experiments,[9-11] takes advantage of the short spin–lattice relaxation times T_1 of the solvated chain segments.[2,12]

For example, Figure 1 shows ^{13}C NMR spectra of polymer I, which is a 1% cross-linked poly(styrene–divinylbenzene) resin in which 12% of the aromatic rings are functionalized with ephedrine moieties. This polymer was

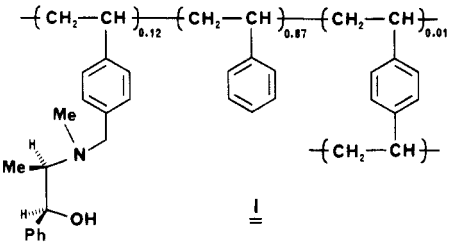

I

prepared by chemical modification of a corresponding chloromethylated resin in which 14% of the aromatic rings carried a chloromethyl group in their para position.[1] As can be seen in Figure 1b, the DP/MAS technique affords excellent signal to noise ratio and reliable representation of all carbon types, comparable to spectra taken[2,6] from soluble polymers.

The corresponding ^{1}H MAS NMR spectrum (Figure 2, curve B) complements the ^{13}C data and demonstrates the chemical utility of this method using high magnetic fields.[8,12,13]

Experimental Section

A Doty Standard 7-mm VT-MAS probe was used with an IBM/Bruker AF-300 spectrometer operating at 75.47 MHz for ^{13}C NMR. Spectra were taken at room temperature in high-resolution mode, using the regular console power through the probe's ^{13}C observe and ^{1}H decouple coils. Shimming to 5-Hz resolution was done on the ^{1}H FID of a 20% $CHCl_3$ in $CDCl_3$ mixture spinning at 1000 Hz. Even better resolution should be achievable with ceramic or Kel-F spacers to restrict the sample volume.

Sapphire rotors with double O-ring sealed Macor end caps (both by Doty) were filled to 40% with the equilibrium-swollen gels under a slight excess of deuteriochloroform. At higher fill rates the combined hydrostatic and vapor pressures would slowly push out the end caps. Spinning rates were 2000 Hz for ^{13}C and 2350 Hz for ^{1}H spectra. No solvent leakage was detected when weighing a chloroform-filled rotor both before and after it was spun at 2000 Hz for 1 h.

The solution-state spectra were taken with a Bruker 5-mm dual tune high-resolution probe with 25-Hz spinning rate. Identical NMR acquisition parameters were used for both 5-mm solution-state and MAS spectra. The solvent resonance at 77.0 ppm and 0.05% tetramethylsilane were used as chemical shift references for ^{13}C and ^{1}H measurements, respectively. The data size was 16K, zerofilled to 32K. Pulse widths were 3 μs for ^{13}C spectra and 2 μs for ^{1}H spectra, corresponding to flip angles of less than 45°. Relaxation delays were 0.3 s (^{13}C) and 2 s (^{1}H). Exponential line broadening of 3 Hz was used for the ^{13}C spectra and none for the ^{1}H spectra. A total of 6150 scans were accumulated for all ^{13}C spectra, with broad-band proton decoupling (1 W).

Results and Discussion

In Figures 1B and 2B we show ^{13}C and ^{1}H DP/MAS NMR spectra of 12% ephedrine-functionalized polymer I. For comparison purposes the corresponding 5-mm solution state spectra of the gel are shown directly above as Figures 1A and 2A. While in the ^{13}C solution-state spectrum (Figure 1A) the superlorentzian backbone signals dominate the aromatic region, MAS line narrowing (Figure 1B) reveals a wealth of smaller aromatic signals. At the same time, the direct polarization technique ensures reliable representation of quaternary and mobile pendant carbons.

The ephedrine phenyl signals can be seen at 142.5 ppm (quaternary) and at 126.1 and 126.9 ppm (*o*- and *p*-CH). The high motional freedom of the pendant ephedrine phenyl makes their signals quite sharp compared to the

0024-9297/89/2222-1574$01.50/0